Sustainability **2014**, *6*, 5535-5553; doi:10.3390/su6095535

OPEN ACCESS

sustainability

ISSN 2071-1050

www.mdpi.com/journal/sustainability

Article

A Sustainable Approach for the Geopolymerization of Natural Iron-Rich Aluminosilicate Materials

Esther A. Obonyo [1], Elie Kamseu [2,3,*], Patrick N. Lemougna [2], Arlin B. Tchamba [2], Uphie C. Melo [2] and Cristina Leonelli [3]

[1] Department of Construction Management, M.E. Rinker School of Building Construction, University of Florida, P.O.Box 115703, Gainesville, FL 32601, USA; E-Mail: obonyo@ufl.edu

[2] Department of research, Local Materials Promotion Authority, MINRESI/MIPROMALO, P.O.Box 2396, Yaoundé 11852, Cameroon; E-Mails: Lemougna@yahoo.fr (P.N.L.); Attchamba@yahoo.fr (A.B.T.); Chinjeuphie@yahoo.co.uk (U.C.M.)

[3] Department of Engineering "Enzo Ferrari", University of Modena and Reggio Emilia, Via Vignolese 905, Modena 41125, Italy; E-Mail: cristina.leonelli@unimore.it

* Author to whom correspondence should be addressed; E-Mail: Kamseuelie2001@yahoo.fr.

Received: 7 July 2014; in revised form: 14 August 2014 / Accepted: 15 August 2014 / Published: 25 August 2014

Abstract: Two iron-rich clayey materials (L1 and L2, with the main difference being the level of iron accumulation) have been studied for their suitability as solid precursors for inorganic polymer composites. L1, with the lower iron content, was calcined at 700°C for 4 h and used as replacement, in the range of 15–35 wt%, for both raw laterites in the formulations of geopolymeric composites. The different mixtures were activated with a highly concentrated alkaline solution containing sodium hydroxide and sodium silicate. River sand with semi-crystalline structure was added to form semi-dry pastes which were pressed to appropriate shape. X-ray diffraction, Infrared spectroscopy, Scanning Electron Microscopy and Mercury Intrusion Porosimetry results demonstrated the effectiveness of the calcined fraction of L1 to act as nucleation sites and extend the geopolymerization to the matrix composites. A highly compact matrix with low porosity and good stability in water, together with a strength comparable to that of standard concretes was obtained allowing for conclusions to be made on the quality of laterites as promising solid precursor for sustainable, environmentally-friendly, and cost-efficient structural materials.

Keywords: iron-rich aluminosilicates; geopolymerization; porosity; mechanical strength

1. Introduction

Laterites and lateritic soils, described as Fe_2O_3-Al_2O_3-SiO_2-H_2O matrices, are made from kaolinite in which a high proportion of Al^{3+} is replaced by Fe^{2+} or Fe^{3+}. This replacement induces important transformation of the structure of the kaolinite: reduction of the crystallinity, increase of the crystal layer and the amorphous phase with consequent increase in the vulnerability to chemical attack [1–5].

Ambrost *et al.* [6], described the antagonism between hematite and kaolinite in the matrix of laterite: the corrosion of the kaolinite is followed by a complete destruction of the crystal giving place to hematite or goethite organized into thin lamellar structures; the crystals of Al-rich hematite or Al-rich goethite formed maintain a clear trace of the shapes of former kaolinite platelets. They postulated that, in the deep layers of laterites fed by Fe^{3+} solutions, the protons necessary to dissolve kaolinite are generated by a reaction similar to the oxidation–hydrolysis step of ferrolysis [6]. Several papers [3–5] have shown that, at the places where iron oxides are invading the pores of a soft clay matrix, this matrix soon becomes corroded. Ambrost *et al.* [6] indicated that the protons released by the precipitation of 1 cm^3 of ferrihydrite may solubilize about 1.5 cm^3 of kaolinite. On the other hand, the precipitation of ferrihydrite from Fe^{3+} solutions has been shown to be accelerated by interfaces such as those of silica or kaolinite particles. In the presence of kaolinite, the release of Al^{3+} species into solution and the precipitation of Fe^{3+} hydroxide were observed to be two simultaneous processes [4–6].

The increase in iron accumulation led to firstly the production of nodule nuclides that progressively grow with the iron content and, finally, laterite concrete is formed with amorphous silica which acts as binder [4–6].The induration of lateritic soils is specific in the tropical regions. The fluctuation of temperature and humidity, grain size, kinetics of precipitation and equilibrium conditions, involving the activity of water, are factors controlling the formation of indurated matrices of laterites. Mottles and concretions with essentially hematite and goethite are a very small size in the first steps of the induration. During the last steps, the goethite phase appears in quite well formed crystals of about 1 micrometer. However, hematite and goethite are generally present with tiny particles of 100 Å, suggesting more impact of dehydration and water activity. For Schwertmann, 1999 [7], rapid release of Fe and low concentration of organic compound favors hematite formation while high concentration of organic compounds favors goethite. For kinetic reasons, goethite is more common than hematite, and also hematite, once appeared, does not rehydrate to form coarse goethite. The driving force of the migration and accumulation of iron will be suggested to be the difference in size of pores which tends to be accentuated as the concretion process [8]. For Schellmann *et al.* [7], the chemical and mineralogical results have shown that the primary minerals are generally not fully dissolved but partially transformed in secondary minerals which are more stable. On the other hand, the iron content of laterites will enhance the kinetic of transformation of kaolinite with structure already affected. Various literature discusses the formation and transformations of ferrihydrite under different chemical conditions [9–11].

It is expected that the disordered structure of the laterites will allow their dissolution in high alkaline solution and the geopolymerization, reaction products of the laterites and laterites soils in alkali activated media will provide mechanical properties comparable to hardened hydrated composites but with significant reduction of greenhouse footprint [12]. It is easier in tropical areas to have laterites, generally at the surface, than struggle for clays for which exploitation will be detrimental for the environment because they are covered in most cases by laterites or various types of soils.

A sustainable material should be locally sourced and produced using renewable resources, with negligible transport costs and environmental impact, having thermal efficiency, financial viability and low energy required in the manufacturing process [12]. These are requirements that can be easily fulfilled with the manufacturing of geopolymers based on laterites rather than metakaolin. In this paper, the understanding of the geopolymerization process adapted to the specific characteristics of laterites is our goal. A suitable production process for stable and durable inorganic polymer cements and composites with good mechanical strength, low porosity and high density achieved on the basis of the local requirements in agreement with the international standards is proposed.

In the case of laterites, it is here necessary to note that the term describes a range of aluminosilicates in which iron accumulation could be at the stage of nodule nuclides, nodules or larger and coarse iron crusts. Their reactivity and behavior during the polycondensation should be linked to the degree of iron accumulation. Taking in account the goethite-diaspore and hematite-corundum profiles describe as solid solutions of crystallized iron-rich oxihydroxides [3–5], the substitution of Al^{3+} in goethite (Al-goethite) and hematite (Al-hematite) are additional parameters that make the particularity of laterites as aluminosilicates, a particularity that may affect the traditional mechanism of geopolymerisation. To the particle size distribution, reactive amorphous/vitreous phase and the Si/Al, key factors governing the suitability of a solid precursor for geopolymerization of classical aluminosilicates, additional elements as the degree of laterization and the form of iron (ferrihydrite, hematite or goethite) should be considered for laterite materials.

It is expected that lateritic soils can be potential candidates as solid precursors for the geopolymerization. The structure of kaolinite already dissolved/destructed by iron accumulation should be favorable for polycondensation. So, even though all the parameters listed here will not be elucidated in this work, hypotheses described in the above introductive part are used to develop geopolymer matrices with the objectives to verify the effective factors affecting the geopolymerization of this class of aluminosilicates. The present study also intends to confirm whether good geopolymeric products can be obtained from laterites or lateritic soils.

2. Materials and Experimental Methods

2.1. Materials

Two samples of laterites were considered for this study, both collected in Yaoundé town in Cameroon: (i) a red soil (from Mvogbetsi, south west of Yaoundé) with very fine nodules commonly used as additive in the fired clay products and for compressed earth blocks, and (ii) a mix of brown and yellowish soil with high proportion of coarse aggregates. The two materials were collected, dried and ground to fine particles (<80 μm) from Nkolbisson, in the south of Yaoundé, Cameroon. A river sand, semi-crystalline matrix with alpha-quartz as principal mineral, was also collected. The sand has particle size < 500 μm. Table 1 shows the chemical and mineralogical compositions of the three solid precursors.

Table 1. Chemical and mineralogical compositions of laterite 1, laterite 2 and river.

	Laterite 1	**Laterite 2**	**River Sand**
TiO_2	1.73	4.38	0.41
Na_2O	0.57	2.37	2.6
SiO_2	46.70	31.7	59.3
CaO	–	–	9.22
Al_2O_3	23.04	10.6	10.7
K_2O	0.13	1.98	2.14
Fe_2O_3	9.68	35.2	3.02
MgO	0.05	0.07	3.02
L.O.I	17.50	11.3	9.12
Minerals	Kaolinite, quartz, ilmenite, hematite, goethite	Kaolinite, quartz, ilmenite, hematite, goethite	Quartz, plagioclase, ilmenite

Laterite from Mvogbetsi, hereafter L1, with $SiO_2/(Al_2O_3 + Fe_2O_3) = 1.43$ can be classified as iron-rich aluminosilicate (lateritic soil). Here, the iron accumulation seems to be at the initial stage where kaolinite maintains a stable and ordered structure. Ngon Ngon *et al.* [4] described the material as clayey laterite; the minerals identified are anatase, halloysite, kaolinite, hematite, goethite, quartz and rutile. The laterite from Nkolbisson, hereafter L2, with $SiO_2/(Al_2O_3 + Fe_2O_3) = 0.68$ is a real ferruginous soil intermediate between the initial stage and the iron crust (Figure 1a). The difference with L1 is that it is not yet at the level of iron crust; the minerals identified are anatase, kaolinite, ilmenite, hematite, goethite and quartz. The degree of dissolution of kaolinite and subsequent iron accumulation are different for L1 and L2 samples, so that it can be assumed they were collected with the consideration that Laterite 2 could be the subsequent stage of the iron accumulation of Laterite 1 (Figure 1).

Figure 1. X-ray diffraction patterns of Laterite 1 and Laterite 2 showing the difference in the amorphous content: k = kaolin, h = hematite, g = goethite.

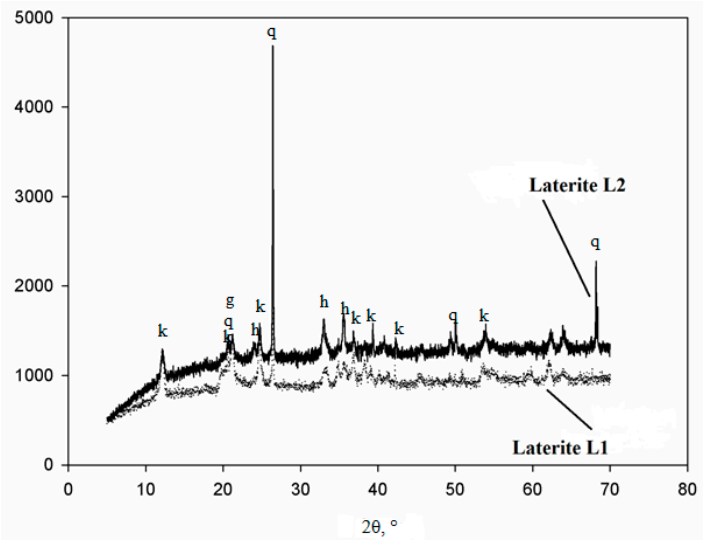

The activation of the solid precursors was done using a mix of sodium hydroxide and sodium silicate in the volume ratio 1:1. The sodium hydroxide (8 M) was prepared by dissolving an appropriate amount of NaOH pellets (99.6 wt%) from Aldrich into deionized water. The sodium

silicate was a high viscous liquid, with SiO_2/Na_2O = 2.99, SiO_2 = 26.45 wt%, Na_2O = 9.14 wt% and L.O.I = 60 wt%, produced by Ingessil, Verona, Italy.

2.2. Compositions Design of Laterite Based Geopolymers

Laterite 1, with high silica content (46.70 wt%), was used to prepare the amorphous fraction of the laterite based geopolymer matrices. Fine powder of Laterite 1 prepared as described above was calcined at 700 °C for 4 h to allow the completion of the loss of structural hydroxyl groups of the residual kaolinite. This amorphous fraction was used from 15–35 wt% on the basis of the literature that describes 3–30 wt% amorphous phase in indurated lateritic blocks [13]. In their work studying the domains of existence of geopolymers, Prud'Homme *et al.* [14] gave similar consideration about the amorphous phase which in their case was between 25 and 40 molar% of soluble silica. They also recognized the impacts of some impurities in the physic-mechanical properties of geopolymers confirming our projection on the use of river sand which here acts as catalytic agents by promoting interfacial reactions and reinforcements. It was not to this extent our intention to speculate on the iron phases, apart from recognizing their action, as described in the literature, in increasing the disorder in kaolinite allowing their reactivity in the geopolymerization context. The formulations were established as described in Table 2.

Table 2. Design of the formulations of laterite based geopolymers.

	$L_1$1	**$L_1$2**	**$L_1$3**	**$L_1$4**	**$L_1$5**	**$L_2$1**	**$L_2$2**	**$L_2$3**	**$L_2$4**	**$L_2$5**
Laterite 1	17	16	15	14	13					
Laterite 2						17	16	15	14	13
Calcined Laterite 1	3	4	5	6	7	3	4	5	6	7
River sand	20	20	20	20	20	20	20	20	20	20
NaH: Na_2SiO_3	9	9	9	9	9	9	9	9	9	9

N.B: the numbers in the table indicate the proportion (wt%) of each component.

2.3. Preparation of Laterite Based Geopolymers

Each powder of laterite prepared was mixed to the appropriate amount of calcined Laterite 1 following the formulation considered (Table 2). River sand was then added and the resultant composite homogenized using ball mill. The alkaline solution was added to the homogeneous powders and a semi-wet pastes obtained. The pastes were pressed using uniaxial type hydraulic press at 40 MPa (Nanneti, Italy). Discs of 40 mm diameter and thickness from 6–9 mm were obtained. The specimens were sealed in plastic for 7 days then the curing continued at room temperature.

2.4. Characterization of Laterites Based Geopolymers

The crystalline phases present in the sintered specimens were identified using the X-ray diffractometer (Philips, mod. PW3710) and a spectroscopy electron microscope (SEM) (Philips mod. XL30). XRD analysis was performed on the flat polished surface to insure the investigations on the real bulk structure of the products. The specimens were scanned from 2θ = 5–70°, at a scanning speed of 2°/min with Cu Kα radiation, λ = 0.154 nm at 40 kV and 40 mA.

Fourier transformed infrared spectroscopy, FT-IR, (Avatar 330 FTIR, Thermo Nicolet) was performed on selected samples analyzing surface and bulk areas. A minimum of 32 scans between 4000 and 400 cm^{-1} were averaged for each spectrum at intervals of 1 cm^{-1}.

For the evaluation of porosity and pore size distribution, we used a Mercury Intrusion Porosimetry (MIP) for its simplicity, quickness and wide measuring range of pore diameter (from 360–0.005 μm in the case under study).

The Mercury Intrusion Porosimeter (MIP) used was an Auto pore IV 9500, 33000 psi (228 MPa) having two low-pressure ports and one high-pressure chamber. Pieces collected from the mechanical test (biaxial flexural strength test) were used to prepare specimens of ~1 cm^3 of volume for the MIP. The sample is weighed and a file is created in which its characteristics are recorded together with analysis conditions and other parameters for the analysis. The measurement includes (1) low-pressure step done with a penetrometer from 0–50 psi (345 kPa), resolution 0.01 psi, pore diameter 360–3.6 μm and transducer accuracy of ±1 of full scale and (2) high-pressure step from atmospheric pressure to 33,000 psi (228 MPa), resolution 0.2 psi from 3000–33,000 psi and 0.1 psi from the atmospheric pressure to 3000 psi, pore diameter 6–0.005 μm and transducer accuracy of ±1 of full scale. When the sample information, analysis conditions, penetrometer properties, and report options are set, the data portion of the sample file is created automatically by the Auto pore software.

The mechanical properties of the laterite based-geopolymer specimens were assessed by the measurement of the biaxial flexural strength through the piston on the three balls test. This test was preferred to the uni-axial bending test because thin plates structures such as structural materials for building and construction are subjected to multi-axial stress states due to complex loading configuration and the geometry structures [15]. The biaxial flexural strength test has an advantage in that it is capable of generating constant equi-axial flexural stress within the area of the loading ring, which is necessary and useful for the investigations of the stochastic nature of the strength of a brittle material [15]. The stress inside the loading ring is identical in all directions, which means cracks would initiate in any direction.

For the piston on the three balls, we modified Kirstein and Woolley's analysis and developed the equation for the maximum biaxial flexural strength:

$$\sigma_{max} = \frac{3P(1+\nu)}{4\pi t^2}\left[1+2\ln\left(\frac{a}{b}\right)+\left(\frac{1-\nu}{1+\nu}\right)\left(1-\frac{b^2}{2a^2}\right)\frac{a^2}{R^2}\right] \quad (1)$$

where P is the ultimate sustained load, a is the radius of the support ring, b is the effective radius of the contact of the loading ball on the specimen, R is the specimen radius, t is the specimen thickness and ν is the Poisson's ratio.

Jihwan *et al.* [15] claimed that this solution should approximately be independent from the number of supporting balls, so it can be applied to axi- but also to non-strictly axi-symmetric testing configurations.

Scanning electron microscopy (SEM) investigations were conducted on a Jeol, mod. 5500 coupled to a EDS probe iXRF system using backscattered electron (BSE) and secondary electron (SE) imaging was used to study the specimens, which were collected from pieces obtained after the biaxial flexural strength test. The fresh fractured pieces were gold coated to ensure conditions of viability for analytical purposes.

3. Results

3.1. Phases Development

Figures 2 and 3 show the X-ray diffraction patterns of the series L1 (b) and L2 (c). The use of river sand is responsible for the predominance of the peaks of alpha-quartz, the principal mineral characterizing the X-ray diffraction patterns. However, focusing on the phases present in the raw laterite [1,4,16] and those from the geopolymers (Figures 2 and 3), it is observed the significant decrease of the peaks of kaolinite (halloysite), goethite and hematite after the geopolymerization. This important decrease is indicative of the extent of geopolymerization of laterites. Hence, for both series (L1 and L2), the peaks of kaolinite/halloysite have almost disappeared due to the dissolution process in high alkaline environment. The residual peaks of kaolinite (halloysite) in the final product of geopolymerization are similar to that of metakaolin based geopolymers since the transformation is generally far from being complete. It is well known that the degree of dissolution of the metakaolin as that of the conversion of kaolinite to metakaolin has never been completed [17,18]. The kaolinite structure is not completely destroyed during the calcination of kaolin. During the activation with alkaline solution, there might be formation of zeolite when the solution does not have enough soluble silica to transform the structure into the amorphous H-N-A-S matrix [18,19]. In the case of laterite based geopolymers, the zeolite formation could be attributed also to the rate of transformation of the disordered kaolinite which is relatively slow allowing competition between the non-crystalline 3D reticulation, *i.e.*, geopolymerization, and the formation of ordered aluminosilicate cages, *i.e.*, zeolite (Figure 1). During the geopolymerization, there will be firstly a rapid dissolution of the calcined fraction of the laterite, and the activated particles of oligomers formed would also act as nucleation sites to extend the dissolution and polymerization across the complete matrix. The residual kaolinite, not completely dissolved, could be then converted to zeolite. Iron accumulation expands the kaolinite layer from 7.2 Å up to 11 Å or more [6]. The hydration of kaolinite present in the laterites and their polycondensation is positively correlated to the degree of stacking disorder created by a given iron accumulation and enhanced by the alkaline context of the geopolymerization. The degree of iron accumulation can define the extent of disorder and the dissolution/polymerization necessary for the classification of laterites for geopolymerization. The interlayer of kaolinite in laterites will be weaker as the iron accumulation is important since the expansion of the kaolinite layer increases the vulnerability in alkaline solution and facilitates their dissolution. The absence of a significant decrease of goethite and hematite could be explained by the unreactive behavior of these minerals in high alkaline media [7,8,10].

Figure 2. X-ray diffraction patterns of Laterite 1 based geopolymers series: q = quartz, h = hematite, g = goethite, * = residual clayey materials.

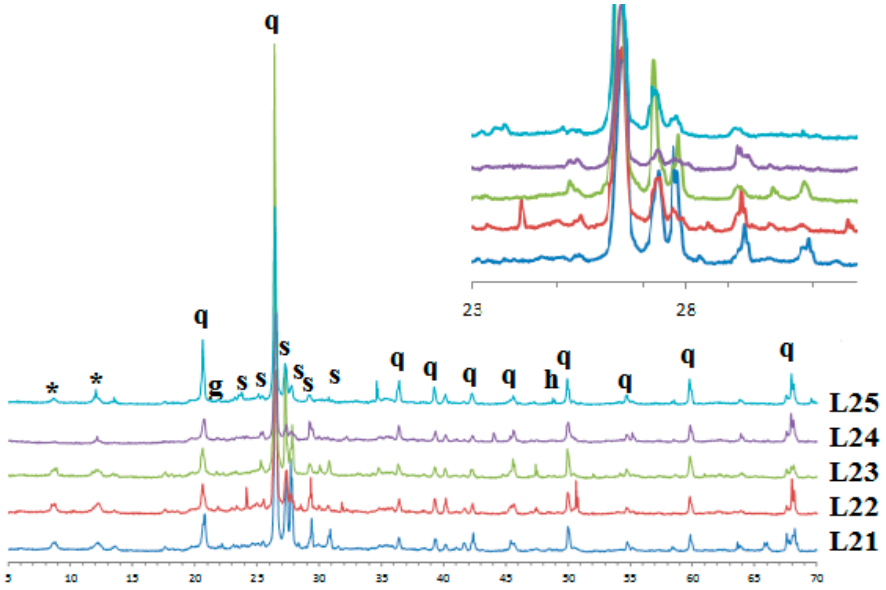

Figure 3. X-ray diffraction patterns of Laterite 2 based geopolymers series: q = quartz, h = hematite, g = goethite, * = residual clayey materials.

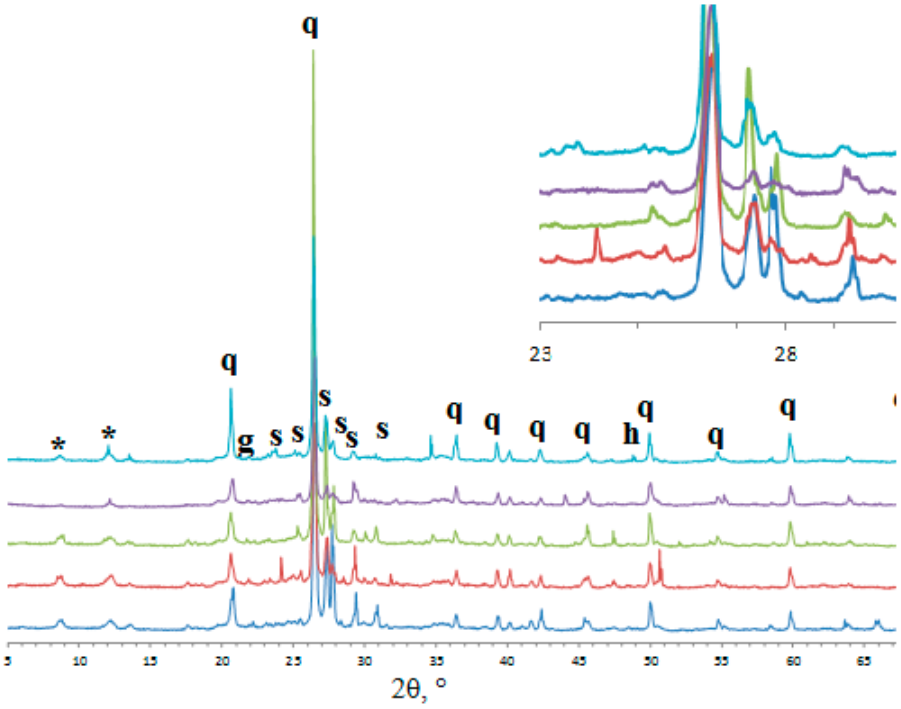

The hydrothermal transformation of the iron oxides and oxyhydroxides via a dissolution—reprecipitation mechanism in aqueous solutions is a common method for the synthesis of colloidal iron oxide phases [10]. The transformation occurs by the dissolution of a less stable form of iron hydrous oxide into ionic (monomers or oligomers) species which then polymerize upon deprotonation or protonation depending on the solution pH. Nucleation and growth of a more stable iron phase then follows [7,8,10]. The disordered kaolinite, the alkaline solution and the calcined laterite, in the context of high alkalinity, are

predominant factors ensuring satisfactory polycondensation. In this situation, the calcined laterite and sodium silicate (with SiO_2/Al_2O_3 ratio appropriate for the reactive fraction) act to facilitate the dissolution/polymerization processes. In both L1 and L2 series (Figures 1–3), important peaks of sodium aluminosilicate hydrates were observed in addition to the broad band/halo characteristic of geopolymeric phases. The predominance of the peaks of alpha-quartz complicates the interpretation of the degree of polymerization. However, the shift of the halo to small 2θ as the expression of the degree of the induration, the compactness of the matrices, porosity, range of pores together with the stability in water contribute to consolidate our suggestions for a sustainable approach in which the semi crystalline structure of the river sand plays a significant role. By increasing the amount of calcined laterite (Figures 1–3), the intensities of the zeolite phase decrease for the series L2 more significantly compared to the series L1. This difference is essentially linked to the kaolinite content in the two samples of laterites, samples for which the degree of iron accumulation is the main difference. The conditions of geopolymerization designed in this study were found suitable for the complete transformation of the series L2. However, the stability of both series demonstrated that zeolites formed here could be contributive for the final structure of geopolymers playing a significant role on the final consolidation. The halo observed in Figure 1 can be correlated to the important IR peak at 993 cm^{-1}, peak characteristics of the H-M-A-S phase (Figure 4). This principal peak is followed by three peaks situated in the interval between 469 cm^{-1} and 798 cm^{-1}: peaks that have been described as the results of geopolymerization of aluminosilicates. The above described peaks correspond to the stretching vibration of the bonds Si-O, Si-O-Al and Al-O. The behavior of the peak at 1460 cm^{-1} is important for the evaluation of the development of carbonates due to the residual silica or unreacted alkali ions. Moreover, the peaks characteristics of water are almost absent indicating that the laterites based inorganic polymers have relatively low water content compared to the standard metakaolin based geopolymers. This can be explained with the presence of iron-based minerals and the silica content. The semi-crystalline structure of the sand allows their incongruent dissolution in the alkaline medium increasing the reactivity with the consequent strength enhancement.

Figure 4. Infrared spectroscopy spectrum of laterite-based geopolymers.

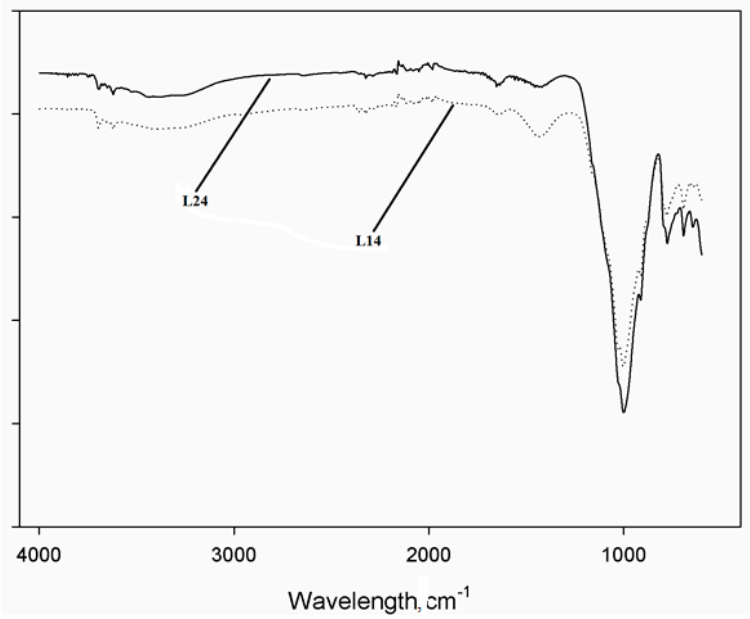

3.2. Porosity, Pore Size Distribution and Water Absorption

The values of water absorption collected after complete curing at 90 days are presented in the Figure 3. It appears that laterites based geopolymers have water absorption ranging from 4%–14%, values relatively low with respect to the metakaolin based geopolymers [20–22]. Water absorption values of the series L1 was 4.5% at 15 wt% of addition of calcined Laterite 1. With the increase of the amount of calcined Laterite L1 from 15–35 wt%, the value of the water absorption oscillated around 7.5%. For the series L2, the water absorption was 10.5% at 15 wt% of addition and remained around 12% with the increase in calcined Laterite L1 (Figure 5). Straightforward correlation was not evident between the water absorption and the calcined laterite content. The major points obtained drawing the variation of the water absorption with addition of calcined L1 fall in a larger interval of band allowing the suggestion that, at the end of the curing, the significance of the calcined laterite was not a limited factor for the permeability of the materials to water. The approach of the production of the laterite based geopolymers (pressing of the wet pastes) and the iron content of raw samples explained the increase of bulk density in relation with the reduction of voids linked to the air bubbles developed during the geopolymerization processes [20–23].

Figure 5. Water absorption of laterite-based geopolymers: series L1 and L2 as function of the calcined L1 added.

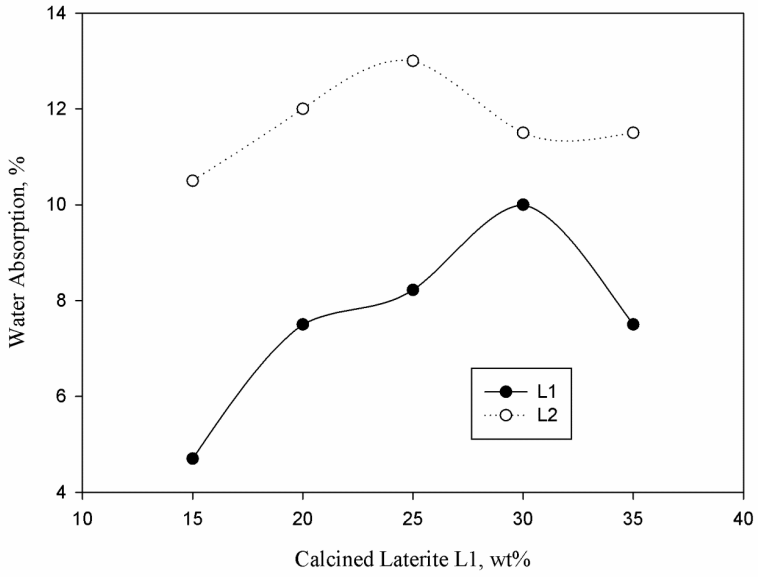

Increasing the calcined laterite content, the kinetics of geopolymerization increased due to the significant changes induced in terms of the amount of solid precursor that can be quickly dissolved, the Si/Al and the iron content change. Considering the bulk density and water absorption for the evaluation of polycondensation, they seem to be linked for the cases under study to the iron content and the extent of dissolution of the solid precursors (essentially the raw laterites and their respective degree of iron accumulation) even though the content of the calcined L1 plays a significant role.

Figure 4 shows the typical cumulative pore volume and the pore size distribution of a fully polycondensed laterite-based geopolymer. The curves evidence the three modes generally described in literature for cement-based materials [20,21,23–25].

Figure 6. Cumulative pore volume (**a**) and pore size distribution (**b**) of laterite L1 and L2 based geopolymers.

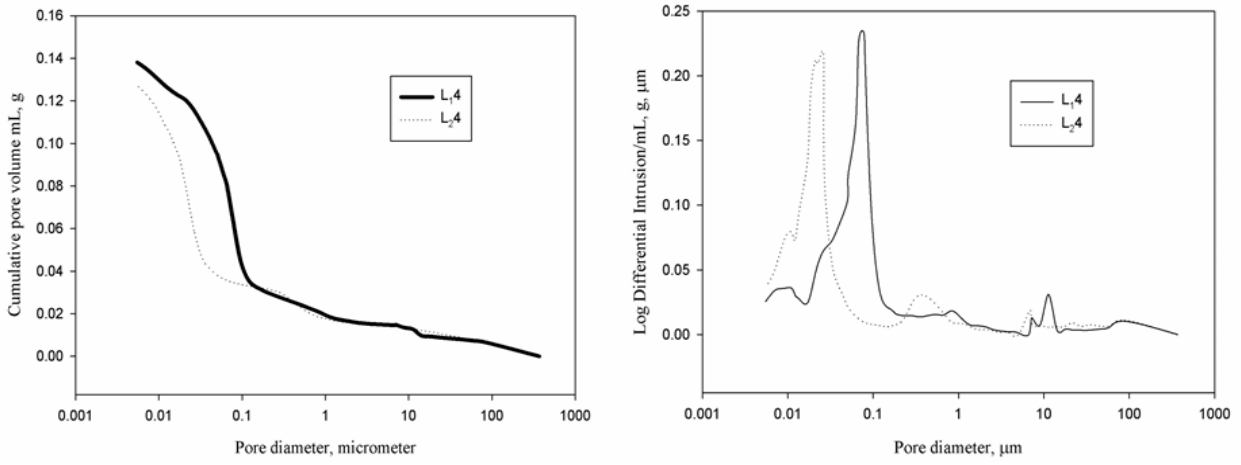

The capillary pores, considered to be made up of water-filled spaces ranging here from 100–200 µm including micro cracks as results of shrinkage due to moisture gradients and the differences in stiffness of materials components. As indicated by Kumar and Bhattacharjee, 2003 [23], capillary porosity is also linked to the degree of hydration and compaction of the mortar. The above described pores are generally called larger capillary pores and are concentrated in the series L1 at 1, 10 and 100 µm; and at 0.5, 1 and 100 µm for L2 series (Figure 6). The larger capillary pores play a significant role in the water permeability of the materials since their drainage has an impact on the continuity of the percolated part of the liquid phase. The small capillary pores are the most important fraction of porosity and are concentrated between 10 and 100 nm for sample L1, and from 10–50 nm for sample L2 (Figure 6). There are still discussions on their action on the permeability and durability of materials. However, the materials obtained here presented a pore threshold of 0.05 µm for L2 and 0.09 µm for L1, far from that of fired bricks (>10 µm) [13]. The gel pores here appeared with mode between 0.005 and 0.01 µm. Due to the porous structure of the H-N-A-S gel with respect to C-S-H gel, it is difficult to express with accuracy the limit between the gel pores and thin capillary pores. The larger and thin capillary pores slightly shifted to lower values for L2 when compared to L1. This shift should be linked to the degree of polycondensation, more important in L2 with respect to L1. The degree of iron accumulation in L2 can explain the high level of disorder and consequent dissolution and polymerization that resulted in the lower presence of zeolite in L2 compared to L1 (Figure 1).

The cumulative pore volume was 0.138 mL/g and 0.127 mL/g for L1 and L2, respectively. These values are relatively low with respect to those generally presented for bricks and conventional concretes [26,27]. Apart from the combined actions of geopolymerization and iron phases, the approach of pressing the geopolymer pastes appeared determinant in reducing the total porosity. Moreover, the compositions' design integrating the river sand allowed the reduction of the air-bubbles and hence, modifying significantly the pore size distribution by shifting the interval of pores to the more fine sizes. This range of pores should surely modify the kinetic of the ingress of fluid into the interior of matrix. Since smaller pores will reduce the ingress, the physical/chemical changes in the

internal structure of the matrix will be not significant and therefore durability can be expected. The parameters of the porosity show 26.74% and 28.32% of pore volume, respectively, for L1 and L2 with 30 wt% of calcined laterites. The cumulative pore volumes of both materials are not far different. However, the bulk density obtained is 1.93 g/mL for L1 and 2.23 g/mL for L2. This significant difference could be linked to the average pore diameter: 0.0405 μm for L1 and 0.0230 μm for L2. It seems that L2 is denser with very fine porosity while L1 has larger pores as already confirmed with the results of Figure 4. The action of iron on the disorganization of kaolinite increases the kinetic of reactions during the geopolymerization, important in interpreting the differences in densification of the two series of inorganic polymer composites.

3.3. Mechanical Properties and Fracture Surface Observations

The fracture surfaces of the laterite based geopolymers presented in the Figure 5 are typically that of the metakaolin based geopolymers [20,21,28].

Figure 7. Fracture surfaces of laterite based geopolymers: L1 (**a**) and L2 (**b**) showing dense matrices comparable to the matrix of metakaolin based geopolymers with some open porosity and heterogeneity (**c)** and (**d**).

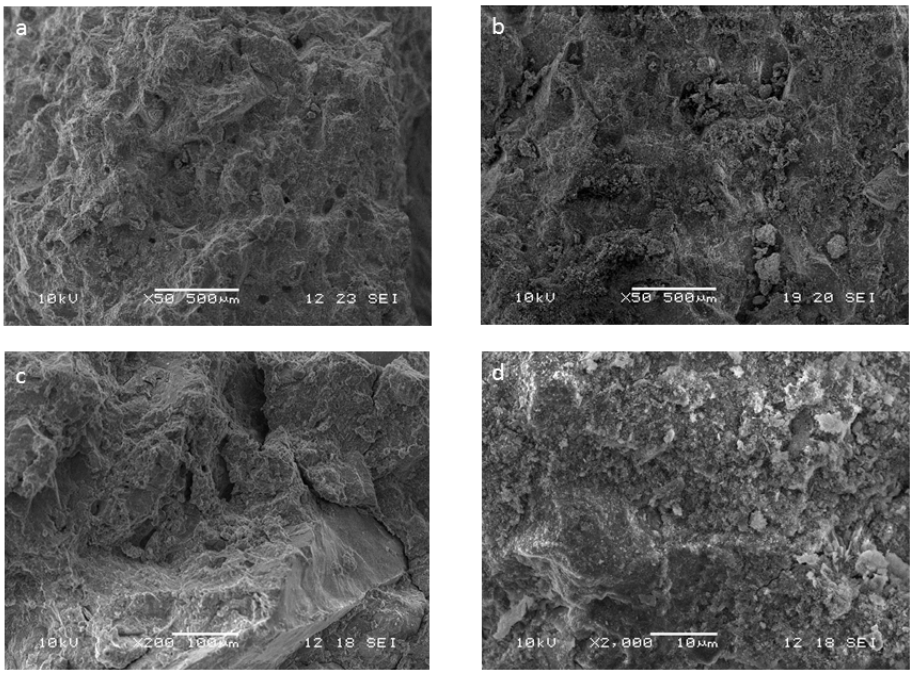

The matrices evidence the coarsening of the microstructure of the geopolymerization products, which were enhanced with the presence of a high proportion of river sand. The river sand increases the possibility of important cross-linking, due to its semi-crystalline structure. The residual pores effects, essentially linked to the air bubbles, are relatively important in L1 (Figure 7a) compared to L2 (Figure 7b). However, the impact of these types of porosity here is less pronounced as the presence of sand and the forming technique used (pressing) do modify considerably the expressions of the formation of bubbles. The SEM micrographs (Figure 7c,d) evidence silica grains embedded in the matrix of geopolymer. The perfect compatibility is due to the semi-crystalline structure of the river sand. Figure 6 demonstrated

more continuity of the matrix L1 (Figure 8a) with respect to L2 (Figure 8b) due to the fact that the Si/Al ratio allows the formation of more H-N-A-S gel capable to fill space available in the concrete structure of laterites matrix.

Figure 8. SEM micrographs showing L1 (**a**) and L2 (**b**) with different densification and pore size distribution as well as fracture behavior due to the difference in the gel content during geopolymerization.

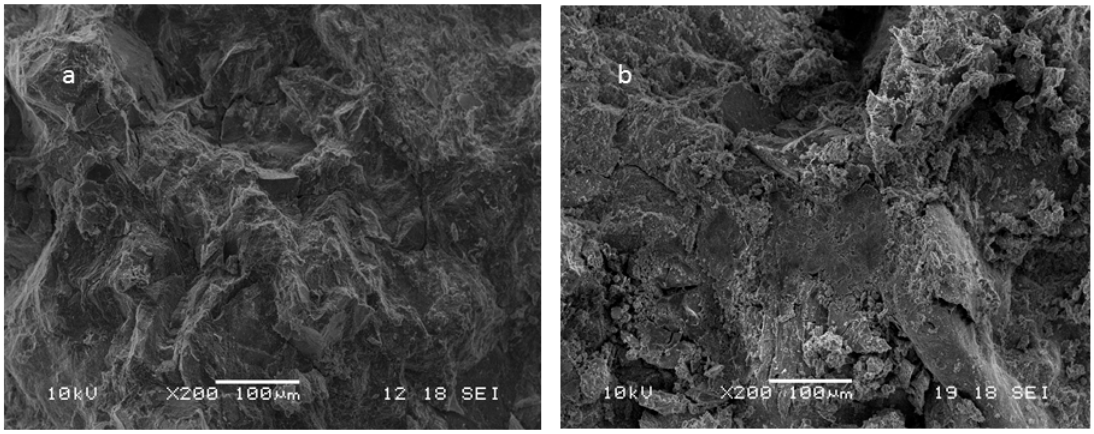

Figure 9 shows the crystallization of H-N-(A)-S phase, non-soluble in water and identified with XRD as zeolite [20,21,29]. The formation of these phases was important in L1 with respect to L2 suggesting the impact of the level of iron accumulation and that of alumina oligomers leached during dissolution. The difference in iron accumulation affects the formation of sodium aluminosilicates; there are decreases in the kinetic of polymerization with the increase in iron content and this is relevant for the interpretation of the chemistry of all the formulations.

Figure 9. SEM micrographs of the laterite based geopolymers showing the phase distributions and their contribution for the densification; a crystalline phase is observed, identified as zeolite.

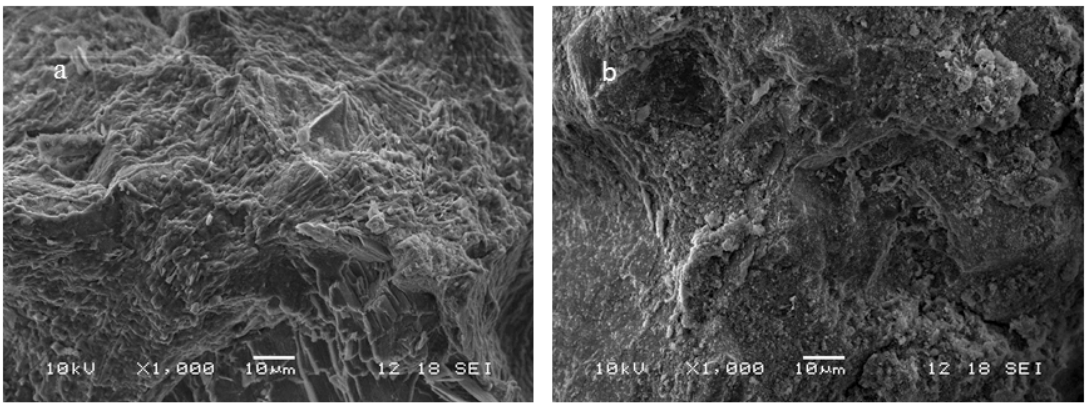

The global trend of the two series L1 and L2 under the bi-axial four points' flexural strength as function of the addition of calcined L1 is presented in Figure 8. Specimens of series L1 present flexural strength from 9–13 MPa. The distribution of the data with the increase of calcined laterite content does not allow drawing straightforward relations between the strength and the amount of

calcined L1. There is an increase in flexural strength between 15 and 20 wt% of calcined laterite; further addition of calcined L1 did not modify the strength. It seems that in this interval, the matrix receives the amount of calcined L1 sufficient to nucleate and develop optimum geopolymerization. For the series L2, the flexural strength was significantly low when less than 25 wt% of calcined L1 was added. In this case, the strength is function of the amount of geopolymeric gel developed capable to embed the matrix phase. The matrix, which is coarser with a high level of iron accumulation, does not have enough binding strength and presents only 6 MPa of flexural strength at 15 wt% of addition, 7 MPa for 20 and 25 wt% of L1 addition. From 30 wt% of calcined L1, 14 MPa of flexural strength was measured indicating the better polycondensation. The results of the bi-axial flexural strength are comparable to those presented by Jihwan *et al.* [15] 2004; Diaz *et al.* [30] 2004, for conventional concretes. The high strength achieved with the laterite based geopolymer products support the reliability of our approach and confirm that the laterites are disordered enough to allow them to participate without previous treatment to the geopolymerization process in high alkaline media. The strengthening mechanism includes the processing method which permits intimate contact between particles and favors the surface reactivity with the fraction of polymerization of alumina and silicate that contribute to the reduction of the porosity and an increase in densification (Figure 10). The lower value water absorption is the result of the limited cumulative pore volume and pore size distribution (Figures 4,9 and 10).

Figure 10. Bi-axial flexural strength of laterites based geopolymers.

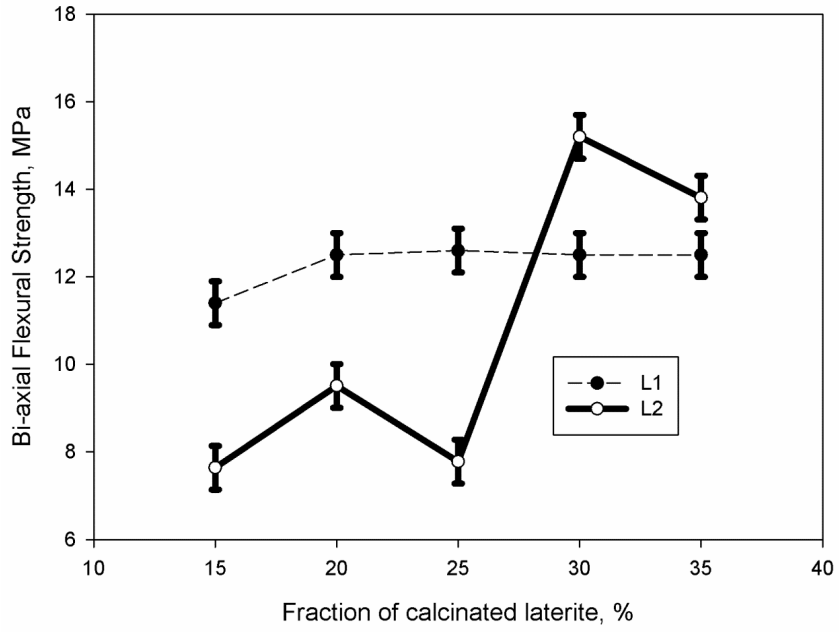

The polycondensation here included the formation of H-N-A-S and the binding action of oxyhydrate and others iron phases active in the geopolymerization environment. The reaction product is a highly cross-linked aluminosilicate gel, which provides mechanical performance to the final matrix comparable to the hardened hydrated cement [26]. The bi-axial flexural strength of 14 MPa for the best formulation is indicative of the effectiveness of laterites and lateritic soils to be used as raw materials for sustainable structural materials.

4. Discussion and Conclusions

The characterization of laterite-based geopolymer composites revealed the effectiveness of sodium aluminium silicates, H-N-A-S, (Figure 1), and sodalite as the principal binder phase formed. The final products presented a good stability in water, low water absorption and mechanical properties comparable to that of conventional concretes. The cumulative pore volume presented by the two series (0.138 mL/g for $L_1$4 and 0.127 mL/g for $L_2$4) were found similar to that of hardened cement paste and lower with respect to bricks from fired clayey materials. The microstructure of the products showed compact structure with fracture surfaces evidencing the cross linking between phases and particles with texture similar to that of high compact composites.

The products of the geopolymerization of laterites showed stability in water already after 14 days and good stability after 90 days indicating the effective transformation and induration of the matrices. This stability varies with the content of calcined laterite and the degree of iron accumulation of the laterite used: the higher the calcined laterite in the formulation (35 wt%), the shorter the period of time needed for stability in water. It should be mentioned that the kinetics of geopolymerization of laterites are slow, surely due to the fact that the disorder in the laterite samples (L1 and L2) is not at the level of metakaolin, fly ash, volcanic ash, *etc*. Nevertheless, the disorder of the structure of aluminosilicate is significant for their dissolution into high alkaline media and, for this reason, even though the kinetic of dissolution and polycondensation is slow, the prerequisites exist and the presence of soluble silica help the polycondensation conduce to the formation of geopolymeric phases. Reducing the curing time by improving the dissolution kinetic could be as significant a contribution to enhance the process and provide the opportunity for it to be competitive in the manufacturing process.

It is important to indicate that the fired clay technology originated from the availability of plastic and low temperature clayey materials in the part of the world where they are abundantly developed. Unfortunately, in the tropical zone, the plastic clayey materials, particularly those suitable for the low temperature bricks and pipes are not the most available and are even rare in some areas. Iron-rich clays, laterites and lateritic soils are the most abundant raw materials in the tropical regions, with an abundance that allows sustainable exploitation while preserving the environment [1,2,4]. In those laterites, hematite, goethite and ferryhydrates are the main secondary phases indicative of the degree of the iron accumulation and their diffusion into the matrix. The iron accumulation in the clayey matrix conducts to the development of a significant disorder in the structure of kaolinite, the principal clay mineral. Another important impact of the iron accumulation is the increase of the kaolinite interlayer distance from 7.2 up to 11 Å. All these considerations motivated our vision of a sustainable approach of the geopolymerization of laterites. The degree of disorder in the laterites is not to compare with that of the metakaolin therefore, we projected a formulation in which 15–35 wt% of laterite has been thermally treated at 700 °C to enhance the structural disorder with the objectives to promote quick dissolution and polymerization that might act in the matrix as nucleating sites and propagate the dissolution/polycondensation.

Iron accumulation plays a major role in the disorganization of the kaolinite, the principal mineral of laterites, providing the alkaline solution the possibility to complete the dissolution and promote polymerization/polycondensation. However, the reaction kinetic was very slow: instead of being 12–16 h, which is generally consistent with the time it takes for a standard metakaolin-based inorganic polymer

cement to complete the transformation of paste to solid matrix, it took more than 72 h for the laterite based inorganic polymer composites to form a strong matrix and more than 60 days to present the maximum strength. With the presence of iron at a significant percentage, the geopolymerization of laterites includes more complex series of reactions as dissolution, diffusion, polymerization and complexation. A temperature slightly higher than that of room temperature is required for the optimization of the reactions. Even though the kinetic of reactions of geopolymerization was not the specific objectives of this work, it was noted that the results described here should be considered for a curing temperature not less than 25 °C and not more than 50 °C. These conditions seem more linked to the iron phase transformations and might be correlated with the conditions described for the induration of laterites where iron plays a significant role [5–9]. The incongruent dissolution of the river sand allows the presence of: (1) soluble silica which is important in enhancing the polycondensation and cross linking between phases and particles; and (2) silicates with rough surface particles that can act as a nucleation site or chemical balance for the equilibrium of the structure.

The strength and water permeability of concretes have been improved by adding Fe_2O_3 nanoparticles in the cement up to 4.0 wt%, with the strengthening mechanism related to the capacity of Fe_2O_3 to act as foreign nucleation site as well as nanofillers recovering the pore structure of the specimens and accelerating the C-S-H gel formation [30,31]. observed that the amount of iron up to 12–14 wt% found in the volcanic ashes was not detrimental for the reactivity and strength development of geopolymers. However, they noted that major part of this iron was concentrated in the crystalline phases as augite and ferroanforsterite [32]. The production of geopolymer from red mud with a high amount of iron (>30 wt%) [29,31] gives relatively low mechanical properties at an earlier stage of the geopolymerization. Geopolymers with 100% Fe designed by Bell *et al.* [33] 2009; Wagh and Douse, 1991 [34], do not reach the complete solidification after a year of curing. In the high alkaline solution with the curing temperature considered for the geopolymerization of laterite based polymer composites, oxyhydrates and goethite are able to transform to more stable iron minerals as hematite, or integrate the structure of the geopolymer. In this direction, the chemistry and mineralogy of iron, their particles size and proportion of amorphous are significant in determining the polycondensation and strength of iron-rich aluminosilicates. The difference in mechanical behavior of the two series with calcined L1 < 25 wt% is consistent with the view that the iron interferes with the reactivity and strength development. The extent of geopolymerization and strength development is essentially linked to the stability of the iron phases and their complete integration in the structure of the inorganic polymer composites. The addition of calcined L1 in L2 should not increase only the amorphous fraction ready for polycondensation but re-equilibrate the Si/Al, Al/Fe and even Si/Fe ratio and by the way improve the gel content that acts in cross-linking the particles: the iron content decreases and the H-M-A-S phases increase. The above mentioned help to validate our approach with the objective to maintain under control the key parameters of polycondensation of laterite based inorganic polymers composites. It appeared that mix-design can be applied for the production of stable and highly resistant composites using laterites and lateritic soils through a sustainable cold chemical process.

Acknowledgments

The authors of this article which to acknowledge the contribution from The Academy of Sciences for the Third World (TWAS): Grant No.: 11-024 RG/CHE/AF/AC-G; UNESCO FR:3240262695.

Author Contributions

The project on geopolymers with laterites was inspired from the collaboration between Prof. Esther A. Obonyo and Dr. Elie Kamseu. The experimentals works took place at the University of Modena, Local Materials Promotion Authority and Rinker School of building and Construction of the University of Florida and involved all the authors indicated in this paper. The writing was done by Dr. Elie Kamseu, Prof. Cristina Leonelli and Prof. Esther Obonyo but all the others authors participated in reviewing the manuscript and discuss the results. All authors read and approved the manuscript.

Nomenclature

$H = H_2O$,
M = Na or K,
$A = Al_2O_3$,
$F = Fe_2O_3$,
$S = SiO_2$,
C = CaO

Conflicts of Interest

The authors declare no conflict of interest.

References

1. Kasthurba, A.K.; Santhanam, M.; Achyuthan, H. Investigation of laterite stones for building purpose from Malabar region, Kerala, SW India—Chemical analysis and microstructure studies. *Constr. Build. Mater.* **2008**, *22*, 2400–2408.
2. Kasthurba, A.K.; Santhanam, M.; Mathews, M.S. Investigation of laterite stones for building purpose from Malabar region, Kerela state, SW India-Part 1: Field studies and profile characterization. *Constr. and Build. Mater.* **2007**, *21*, 73–82.
3. Trolard, F.; Tardy, Y. A model of Fe^{3+}-Kaolinite, Al^{3+}-Goethite, Al^{3+}-Hematite equilibria in laterites. *Clay Miner.* **1989**, *24*, 1–21.
4. Ngon Ngon, G.F.; Yongue-Fouateu, R.; Bitom, D.L.; Bilong, P. A geological study of clayey laterite and clayey hydromorphic material of the region of Yaoundé (Cameroon): A prerequisite for local material promotion. *J. Afr. Earth Sci.* **2009**, *55*, 69–78.
5. Nahon, D. Curasses ferrugineuses et encoutements calcaires au Sénégal Occidental et en mauritanie, Systémes évolutifs: Géochimie, structures, relais et coexistence. *Sci. Geol. Mém*. **1976**, *44*, 232. (In French)

6. Ambrost, J.P.; Nahon, D.; herbillon, A.J. The epigenetic replacement of kaolinite by hematite in laterite-petrographic evidence and the mechanisms involved. *Geoderma* **1986**, *37*, 283–294.
7. Schwertmann, U.; Friedl, J.; Stanjek, H. From Fe(III) ions to ferrihydrite and then to hematite. *J. Colloid Interface Sci.* **1999**, *209*, 215–223.
8. Schellmann, U.; Schulze, D.G.; Murad, E. Identification of ferrihydrite in soils by dissolution kinetics, differential X-ray diffraction, and Mossbauer spectroscopy. *Soil Sci. Soc. Am. J.* **1982**, *46*, 869–875.
9. Domingo, C.; Rodriguez-Clemente, R.; Blesa, M.A. Kinetics of oxidative precipitation of iron oxide particles, Colloids and Surfaces. *A-Physicochem. Eng. Aspects* **1993**, *79*, 177–189.
10. Hong, P.V.; Samuel, S.; Loredana, B.; Liane, G.B. Crystallization of hematite (α-Fe_2O_3) under Alkaline condition: The effects of Pb. *Cryst. Growth Des.* **2010**, *10*, 1544–1551.
11. Murray, J.; Kirwan, L.; Loan, M.; Hodnett, B.K. In-situ synchrotron diffraction study of the hydrothermal transformation of goethite to hematite in sodium aluminate solutions. *Hydrometallurgy* **2009**, *95*, 215–223.
12. Duxson, P.; Provis, J.L.; Lukey, G.C.; van Devanter, J.S.J. The role of inorganic polymer technology in the development of green concrete. *Cem. Concr. Res.* **2007**, *37*, 1950–1957.
13. Balbir, S.; Gilkes, R.J. The recognition of amorphous silica in indurated soil profiles. *Clay Miner.* **1993**, *28*, 461–474.
14. Prud'Homme, E.; Autef, A.; Essaidi, N.; Mechaud, P.; Samet, B.; Joussein, E.; Rossignol, S. Defining existence domains in geopolymers through their physicochemical properties. *Appl. Clay Sci.* **2013**, *73*, 26–34.
15. Jihwan, K.; Dong, J.K.; Goangseup, Z. Improvement of the biaxial flexure test method for concrete. *Cem. Concr. Compos*. **2013**, *37*, 154–160.
16. David, C.C.; David, W.R. *Mechanical Testing Methodology for Ceramic Design and Reliability*; Marcel Dekker: New York, NY, USA, 1998; pp. 140–141.
17. Lecomte-nana, G.L.; Lesueur, E.; Bonnet, J.P.; Lecomte, G. Characterization of a lateritic geomaterial and its elaboration through a chemical route. *Constr. Build. Mater.* **2009**, *23*, 1126–1132.
18. Zhang, Z.; Wang, H.; Provis, J.L.; Bullen, F.; Reid, A.; Zhu, Y. Quantitative kinetic and structural analysis of geopolymers. Part 1. The activation of metakaolin with sodium hydroxide. *Thermochim. Acta* **2012**, *539*, 23–33.
19. Zhang, Z.; Provis, J.L.; Wang, H.; Bullen, F.; Reid, A. Quantitative kinetic and structural analysis of geopolymers. Part 2. Thermodynamics of sodium silicate activation of metakaolin. *Thermochim. Acta* **2013**, *539*, 163–171.
20. Kamseu, E.; Bignozzi, M.C.; Melo, U.C.; Leonelli, C.; Sglavo, V.M. Design of inorganic polymer cements: Effects of matrix strengthening on microstructure. *Constr. Build. Mater.* **2013**, *38*, 1135–1145.
21. Kamseu, E.; Leonelli, C.; Chinje, U.M.; Perera, D.S.; Lemougna, P.N. Polysialate Matrixes from Al-Rich and Si-Rich Metakaolins: Polycondensation and Physico-Chemical Propertie. *Interceram* **2011**, *60*, 25–31.
22. Elimbi, A.; Tchakoute, H.K.; Kondoh, M.; Dika, M.J. Thermal behavior and characteristics of fired geopolymers produced from local Cameroonian meta kaolin. *Ceram. Int.* **2014**, in press.
23. Kumar, R.; Bhattacharjee, B. Porosity distribution and *in situ* strength of concrete. *Cem. Concr. Res.* **2003**, *33*, 155–164.

24. Davidson, L.E.; Shaw, S.; Bryan, N.D.; Livens, F.R. The kinetics and mechanisms of schwertmannite transformation to goethite and hematite under alkaline conditions. *Am. Mineral*. **2008**, *93*, 1326–1337.
25. Ranaivomanana, H.; Verdier, J.; Sellier, A.; Bourbon, X. Prediction of relative permeabilities and water vapor diffusion reduction factor for cement-based materials. *Cem. Concr. Res.* **2013**, *48*, 53–63.
26. Zhou, J.; Ye, G.; van Breugel, K. Characterization of pore structure in cement-based materials using pressurization—Depressurization cycling mercury intrusion porosimetry (PDC-MIP). *Cem. Concr. Res.* **2010**, *40*, 1120–1128.
27. Katrin, R.; Dirk, H. Characterization of Mineral Building Materials by Mercury-Intrusion Porosimetry. *Part. Part. Syst. Charact.* **2006**, *23*, 20–28.
28. Kuenzel, C.; Neville, T.P.; Donatello, S.; Vandeperre, L.; Boccaccini, A.R.; Cheeseman, C.R. Influence of metakaolin characteristics on the mechanical properties of geopolymers. *Appl. Clay Sci*. **2013**, *83*, 308–314.
29. He, J.; Jie, Y.; Zhang, J.; Yu, Y.; Zhang, G. Synthesis and characterization of red mud and rice husk ash-based geopolymer composites. *Cem. Concr. Compos*. **2013**, *37*, 108–118.
30. Diaz, B.; Joiret, S.; Keddam, M.; Novoa, X.R.; Perez, M.C.; Takenouti, H. Passivity of iron mud's water solutions. *Electrochem. Acta* **2004**, *49*, 3039–3048.
31. Lemougna, P.N.; Kenneth, J.D.; Mackenzie, J.G.N.; Rahier, H.; Chinje, M.U.F. The role of iron in the formation of inorganic polymers (geopolymers) from volcanic ash: A 57 Fe Mossbauer spectroscopy study. *J. Mater. Sci*. **2013**, *48*, 5280–5286.
32. Khoshakhlagh, A.; Nazari, A.; Khalaj, G. Effects of Fe_2O_3 nanoparticles on water permeability and strength assessments of high strength self-compacting concrete. *J. Mater. Sci. Technol.* **2012**, *28*, 73–82.
33. Bell, J.L., Kriven, W.M., Singh, D., Kriven, W.M., Eds. *Mechanical Properties and Performance of Engineering Ceramics and Composites IV*; Wiley: Hoboken, NJ, USA, 2009; pp. 301–312.
34. Wagh, A.S.; Douse, V.E. Silicate bonded unsintered ceramics of Bayer process waste. *J. Mater. Res.* **1991**, *6*, 1094–1102.